Towards high-efficiency POLO IBC solar cells based on a PERC+ processing technology

Thorsten Dullweber[1], Verena Mertens[1], Maximilian Stöhr[1], Jonathan Langlois[1], Larissa Mettner[1], Ulrike Baumann[1], Felix Haase[1], Rolf Brendel[1,2], Joris Libal[3], Aaron Vogt[4], Norbert Ambrosius[4], Thomas Pernau[5], Helge Haverkamp[5]

[1]Institute for Solar Energy Research Hamelin (ISFH); [2]Institute of Solid-State Physics; [3]ISC Konstanz; [4]LPKF Laser & Electronics AG and [5]centrotherm international AG

Abstract

We develop a novel manufacturing process sequence for polysilicon on oxide (POLO) IBC solar cells by applying a local PECVD SiOxNy/n-a-Si deposition through a glass shadow mask to form the structured carrier-selective n-poly-Si emitter in a single process step. The other POLO IBC processing steps such as AlOx/SiN surface passivation, laser contact opening and Ag and Al screen printing are very similar to those of today's bifacial PERC+ cells, thereby targeting a very cost-competitive manufacturing process. POLO IBC precursors without metal contacts exhibit an excellent implied Voc (iVoc) of 741 mV. The first fully processed POLO IBC cells on M2-sized Ga-doped Cz wafers achieve conversion efficiencies of up to 23.0% with Voc = 708 mV, Jsc = 41.2 mA/cm2 and FF = 78.7%. The 33 mV difference between iVoc and Voc is caused by additional Jo contributions of the Ag and Al metal contacts, which we will improve in the future. These initial results have been obtained by applying a lab-type PECVD tool for the SiOxNy/n-a-Si deposition through shadow masks. Afterwards, we transfer the process to a mass-production c.plasma PECVD tool from centrotherm, which is installed at the ISFH SolarTeC, delivering very promising results also outlined in this paper. As next steps towards production readiness, we aim at further increasing the POLO IBC conversion efficiency towards 25% and implementing an automated shadow mask loading into the industrial c.plasma tool.

Introduction

The global photovoltaics market today is still mostly based on monofacial PERC or bifacial PERC+ solar cells [1]. In mass production, PERC and PERC+ cells achieve conversion efficiencies of around 23% by applying a best-in-class and cost-effective manufacturing process [1]. Nevertheless, the carrier recombination in the phosphorus-doped emitter and at the Ag front contacts limits the Voc and efficiency potential of PERC+ cells to below 700 mV and 24%, respectively [2].

Applying a new model for carrier selectivity [3], ISFH developed the POLO IBC cell [3,4] as next-generation cell technology. The POLO IBC cell design builds on today's industrial PERC+ cells by continuing to use Ga-doped Cz wafers, an AlOx/SiNy rear passivation and Al finger base contacts. However, it replaces the efficiency-limiting phosphorus emitter with a carrier-selective POLO [3,5] contact on the rear side, thereby drastically increasing the Voc potential up to 733 mV with an efficiency potential of up to 25.5%, as confirmed by Quokka simulations [6]. As process technology for POLO IBC cells, ISFH developed a PECVD SiO_xN_y/n-a-Si deposition process for the POLO stack using a lab-type tool with N2O in-situ plasma oxidation, resulting in an excellent passivation quality after firing with J_o = 2 fA/cm² [7]. Glass-based shadow masks enable the confined local PECVD deposition of the SiON/n-a-Si layer stack onto the silicon wafer [8], thereby facilitating a very lean POLO IBC process sequence, as proposed in [9,10].

"The POLO IBC cell design builds on today's industrial PERC+ cells...."

This paper is an abridged version of a recent conference contribution [11], where we report the first fully processed POLO IBC cells, based on local PECVD SiO_xN_y/n-a-Si deposition through a shadow mask, applying a lab-type single-wafer as well as a mass-production type PECVD tool, yielding conversion efficiencies of up to 23.0%. Our cost calculations demonstrate that POLO IBC cells manufactured with this process can be cost-competitive against today's mainstream PERC+ cells.

PECVD SiOxNy/n-a-Si process development and transfer

We have developed a PECVD process to deposit the SiO_xN_y/n-a-Si layer stack in-situ in one deposition process, as published in [7], using a lab-type single wafer tool (Clustertool, Von Ardenne). The lab PECVD tool applies a capacity-coupled plasma source, an in-situ plasma oxidation using N2O to grow an approximately 1.7 nm-thin SiO_xN_y, and SiH4, PH3 and H2 to deposit a 120 nm-thick in-situ-doped n-a-Si layer. To assess the passivation quality, symmetrical n-type Cz test wafers are processed with the PECVD SiO_xN_y/n-a-Si, followed by annealing in N2 at 850°C, PECVD deposition of a 100-nm thick SiNx layer and firing

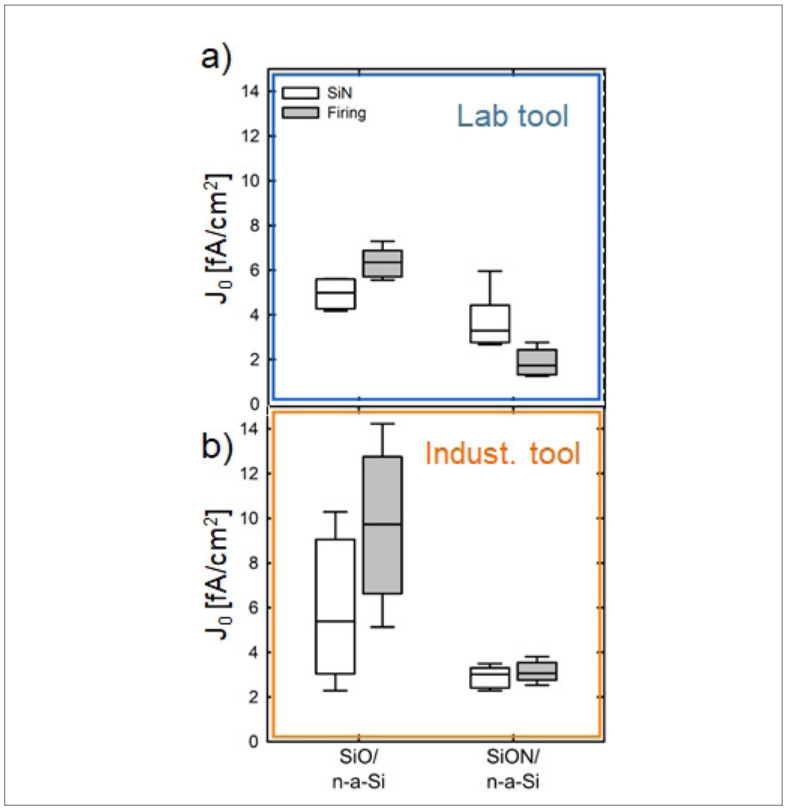

Figure 1: Saturation current density J_0 of symmetrical test wafers passivated with either SiOx/n-a-Si or SiO_xN_y/n-a-Si. Both a) the lab PECVD tool and b) the industrial PECVD tool achieve excellent J_0 values after firing of 2 and 3 fA/cm², respectively, when applying the interfacial SiO_xN_y. In contrast, when using an SiO_x either by a) thermal oxidation or b) plasma oxidation, the surface passivation degrades after firing to J_0 values of 6 and 10 fA/cm², respectively.

at 810°C. Figure 1 a) shows the results obtained with the lab tool, as published in [7], where the SiO_xN_y interface exhibits excellent firing stability in contrast to a thermal SiOx interface, which slightly degrades during firing.

After adapting, implementing and optimising the PECVD SiO_xN_y/n-a-Si recipe to an industrial c.plasma tool from centrotherm at the ISFH SolarTeC (see Figure 2), this tool also achieves very good J_0 values of 3 fA/cm² after firing, as displayed in Figure 1 b). For comparison, we develop an in-situ plasma oxidation using O2 at the industrial tool. As shown in Figure 1 b), the PECVD SiOx/n-a-Si layer stack exhibits higher J_0 values of 6 fA/cm² after SiN deposition, which degrade to 10 fA/cm² after firing. Hence, for both tools, the SiO_xN_y interface grown by in-situ N2O plasma oxidation delivers the best J_0 values after firing. A TEM study confirms that the N2O plasma oxidation incorporates nitrogen at the c-Si / SiO_xN_y interface [11]. It has been shown for SiN layers that nitrogen increases the silicon-to-hydrogen bonding energy, thereby reducing the hydrogen outdiffusion during firing [12]. Similarly, nitrogen at the c-Si / SiO_xN_y interface could increase the hydrogen bonding energy to silicon bonds, thereby contributing to the improved firing stability demonstrated in Figures 1 a) and b).

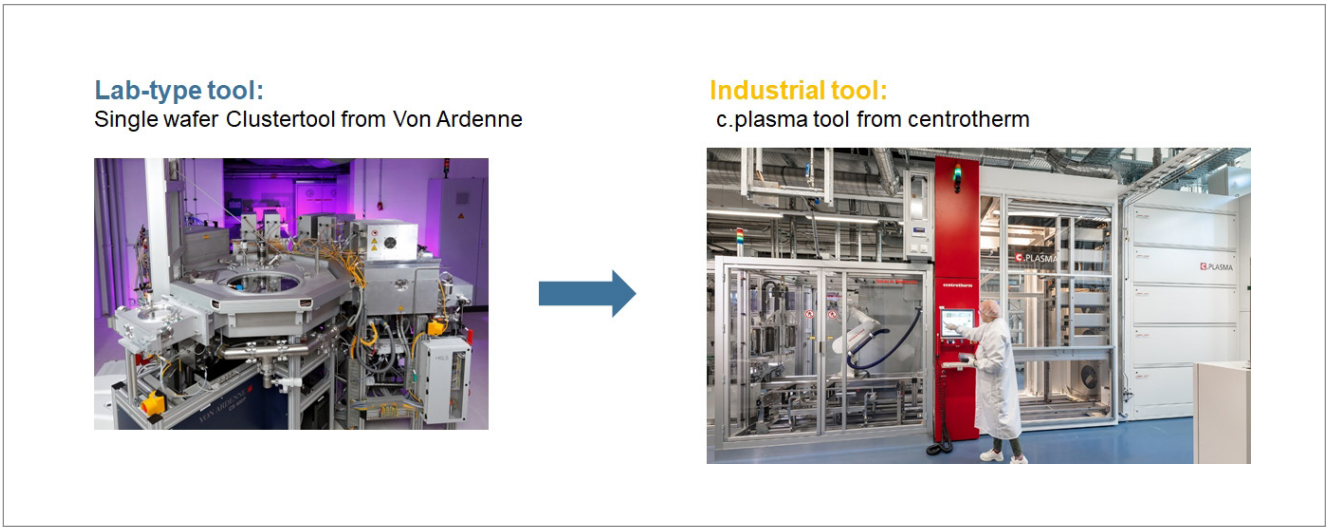

Figure 2: Development of the in-situ PECVD deposition of the $SiOxN_y$/n-a-Si layer stack began with the lab-type tool (left image). After initial promising results, we transferred and adopted the PECVD $SiOxN_y$/n-a-Si recipe to the industrial c.plasma tool at the ISFH SolarTeC (right image).

POLO IBC cells with shadow masks

3.1 Process sequence with shadow masks

The POLO IBC process flow applying the local PECVD SiO_xN_y/n-a-Si deposition through a glass shadow mask is shown schematically in Figure 3. At the beginning, 1Ωcm Ga-doped M2-sized Cz wafers are textured on both sides and subsequently polished on the rear side according to step 1 in Figure 3. Afterwards, we locally deposit the SiO_xN_y SiO_xN_y/n-a-Si layer stack through a glass shadow mask provided by LPKF, by using either the lab-type PECVD tool or the industrial PECVD tool. Step 2 in Figure 3 is completed by annealing the wafers in a nitrogen atmosphere at 850°C. Both sides of the wafer are passivated by an AlOx/SiN layer stack (step 3), followed by laser contact opening (LCO) of the AlOx/SiN at the rear-side base region (step 4). Finally, the Al contacts are screen-printed on top of the LCOs and the Ag contacts are printed aligned to the n-poly-Si. The process sequence is completed by firing the wafers at around 810°C, where the Al contacts locally alloy with the silicon wafer forming an Al-BSF and the Ag paste dissolves the AlOx/SiN layer contacting the n-poly-Si. Compared to an industrial PERC+ process, this POLO IBC process uses the same steps of texturing, rear polishing, AlOx/SiN deposition, LCO, and screen-printing of Al and Ag pastes. Only the POCl3 diffusion and laser doping is replaced by the local PECVD SiO_xN_y/n-a-Si deposition; see also the step-by-step process flow comparison in the cost calculation displayed in Figure 7.

A photograph of an M2-sized glass shadow mask in front of a Cz wafer, which received the local SiO_xN_y/n-a-Si deposition, is displayed in Figure 4 a). A close-up image by light microscopy in Figure 4 b) reveals that the local SiO_xN_y/n-a-Si layer width matches the shadow mask layout within an accuracy of ± 10 µm. Figure 4 c) displays a light microscope image of the rear side of a fully processed POLO IBC cell including screen-printed Al and Ag fingers, which are well aligned to the local SiO_xN_y/n-a-Si layers within an accuracy of ± 20 µm.

"...the SiOx Ny interface exhibits excellent firing stability..."

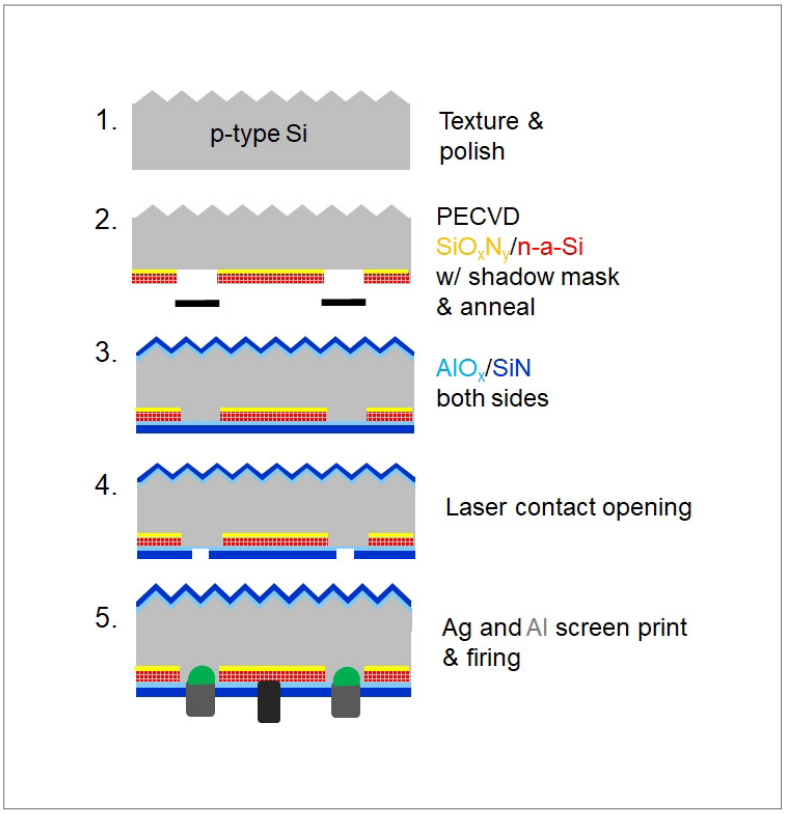

Figure 3: Schematic drawings of the lean POLO IBC process flow applying the local PECVD SiO_xN_y/n-a-Si deposition through a glass shadow mask. All other processing steps are very similar to today's PERC+ solar cell technology.

3.2 Implied Voc results of POLO IBC precursors without metal contacts

We process implied Voc (iVoc) precursors according to the process flow in Figure 3 up to step 3, in order to assess the Voc potential of the POLO IBC cells. We skip LCOs (step 4) and screen-printing (step 5), but apply firing to the iVoc precursors. When depositing the local PECVD SiO_xN_y/n-a-Si layer in the lab-type tool, we obtain excellent average iVoc values of 741 mV determined by infrared lifetime mapping (ILM), as shown in Figure 5. This high iVoc corresponds to a total J_o of 10 fA/cm² of the POLO IBC precursor, revealing the excellent passivation qualities of the local SiO_xN_y/n-a-Si and AlO_x/SiN layers, as well as a very low J_o,bulk of the Ga wafer, which is in accordance with the simulations in [7]. Applying the industrial PECVD tool for the local SiO_xN_y/n-a-Si deposition, we obtain average iVoc values of 721 mV, as shown in Figure 5. However, these wafers have not yet received the optimised PECVD SiO_xN_y/n-a-Si recipe in Figure 1 b), but a previous recipe exhibiting higher J_o values. When applying the improved recipe of Figure 1 b), we expect that the iVoc values of POLO IBC precursors processed in the industrial tool will approach the high iVoc values obtained with the lab-type tool.

3.3 POLO IBC cell results using shadow masks

First, we have processed POLO IBC cells in two subsequent batches using the lab-type PECVD tool as well as a first cell batch using the industrial PECVD tool. The cells are measured with an IV tester (LOANA from pv tools) at ISFH, which uses contact bars to contact the busbars at full length at the rear side of the cells and includes sense pins to measure the voltage of the cell. The illumination is calibrated using the internal calibration of the IV tester, since we do not yet have a POLO IBC cell measured at a certified calibration lab.

The efficiency of IV parameters, open circuit voltage (Voc), short circuit current (J_{sc}) and fill factor (FF) of POLO IBC cells from the second run using the lab-type tool for local PECVD SiO_xN_y/n-a-Si deposition through a shadow mask are displayed in Figure 6. On average, we obtain 22.8% efficiency and Voc = 712 mV. The best POLO IBC cell of this run exhibits a conversion efficiency of 23.0% with Voc= 708 mV, J_{sc} = 41.2 mA/cm² and *FF* = 78.7%. We attribute the 29 mV difference between iVoc = 741 mV (see Figure 5) and Voc = 712 mV to the high Al and Ag contact area fractions of approximately 3% and 10%, respectively. When assuming a typical J_o,Al-BSF of 500 fA/cm² [2]

and J_{0},Ag of 150 fA/cm², the full metallisation would account for an area-weighted J_{0},met of 30 fA/cm², which explains the delta between the measured Voc and iVoc. By reducing the metal area coverage and by further improving the Ag contact properties, we expect to achieve higher Voc values and higher conversion efficiencies in the near future.

The POLO IBC cells using the industrial PECVD tool were processed in two different split groups. Split group 1 received the full PECVD SiO_xN_y/n-a-Si deposition through the shadow mask. Split group 2 received a wet chemically grown SiOx interface by O3 dissolved in DI water, followed by depositing the PECVD n-a-Si layer through the shadow mask. Figure 6 shows the POLO IBC cell results obtained with split 2 using the wet chemical SiOx interface and the local PECVD n-a-Si. We obtained average efficiencies of 21.8% and Voc values of 710 mV with a best cell efficiency of 22.3%. The split with the full PECVD SiO_xN_y/n-a-Si deposition through the shadow mask is not shown in Figure 6. The resulting Voc and J_{sc} values are very similar but the *FF* is significantly lower, which we attribute to the PECVD SiO_xN_y being too thick. We are currently optimising the SiO_xN_y thickness for the industrial tool and will apply it in combination with the improved PECVD SiO_xN_y/n-a-Si recipe of Figure 1 b) to the next POLO IBC cell run. Thereby, we expect that the conversion efficiencies obtained with the industrial tool will approach the values obtained with the lab tool.

Cost assessment of POLO IBC solar cells manufactured with shadow masks

Here, we compare the cost of ownership of each cell manufacturing step using a cost model from ISC Konstanz, as shown in Figure 7, in order to assess the future economic competitiveness of POLO IBC cells manufactured with shadow masks versus today's mainstream PERC+ cells. Assuming M6 wafer size, 5 GWp production in EU and Ag paste costs of 700 US$/kg, we calculate the POLO IBC cell processing costs to be 4.6 US$cent/Wp, applying the cost of ownership values per process step as shown in Figure 7 and assuming a POLO IBC cell efficiency of 25%. As a benchmark, 23% efficient PERC+ cells are currently costed very similarly at 4.5 US$cent/Wp. The marginally higher processing costs of POLO IBC originate from the PECVD SiO_xN_y/n-a-Si process, which is more expensive than the POCl3 diffusion used for PERC+. Based on preliminary experimental results, we target that one shadow mask can be used for about 1000 subsequent PECVD depositions and hence only minimally contributes to the PECVD SiO_xN_y/n-a-Si processing costs.

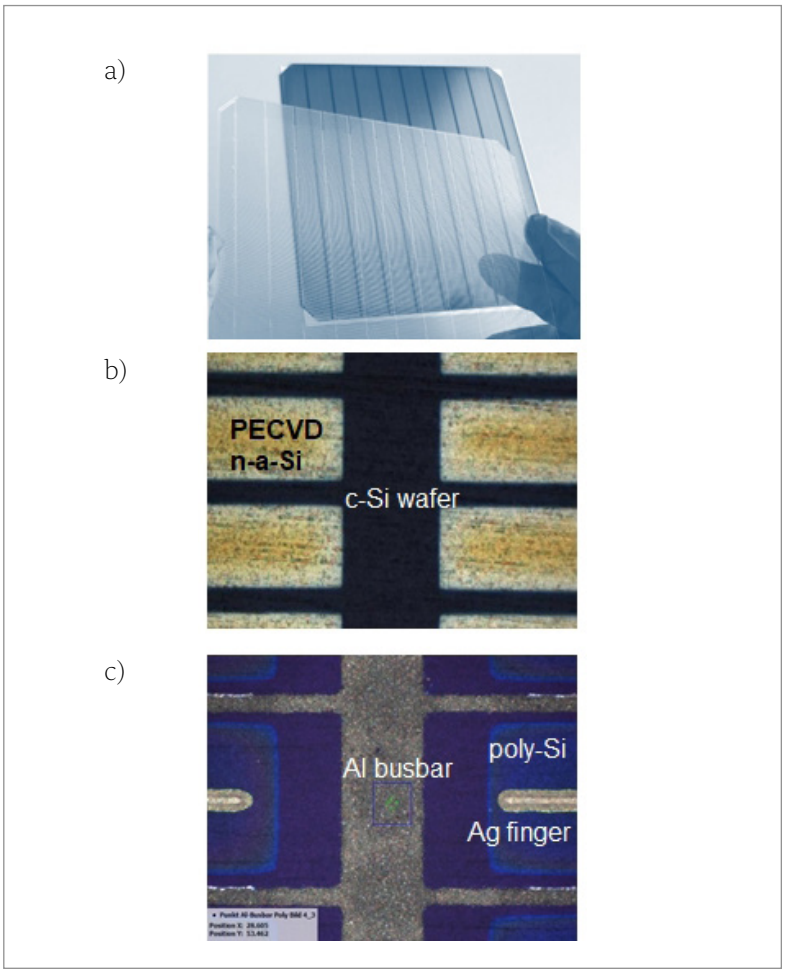

Figure 4: a) Photograph of an M2-sized glass shadow mask in front of a Cz wafer with local SiO_xN_y/n-a-Si layer stack. b) Light microscope image of a local SiO_xN_y/n-a-Si layer stack deposited through the shadow mask in the industrial PECVD tool. c) Light microscope image of the rear side of a fully processed POLO IBC cell including screen-printed Al and Ag fingers, which are well aligned to the local SiO_xN_y/n-a-Si layers.

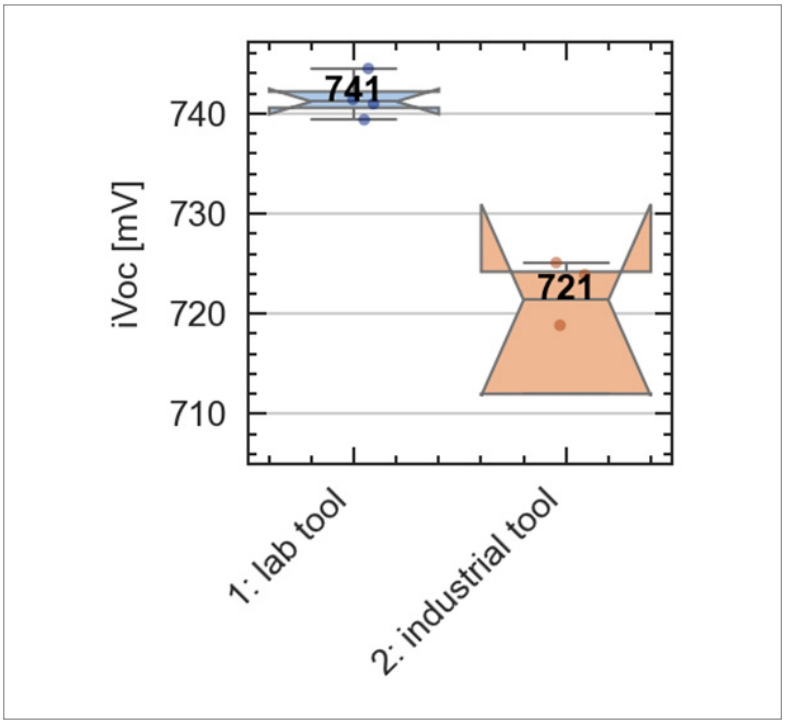

Figure 5: iV_{oc} values of POLO IBC precursors without metal contacts where the local PECVD SiO_xN_y/n-a-Si deposition was performed in the lab tool (group 1) or the industrial tool (group 2).

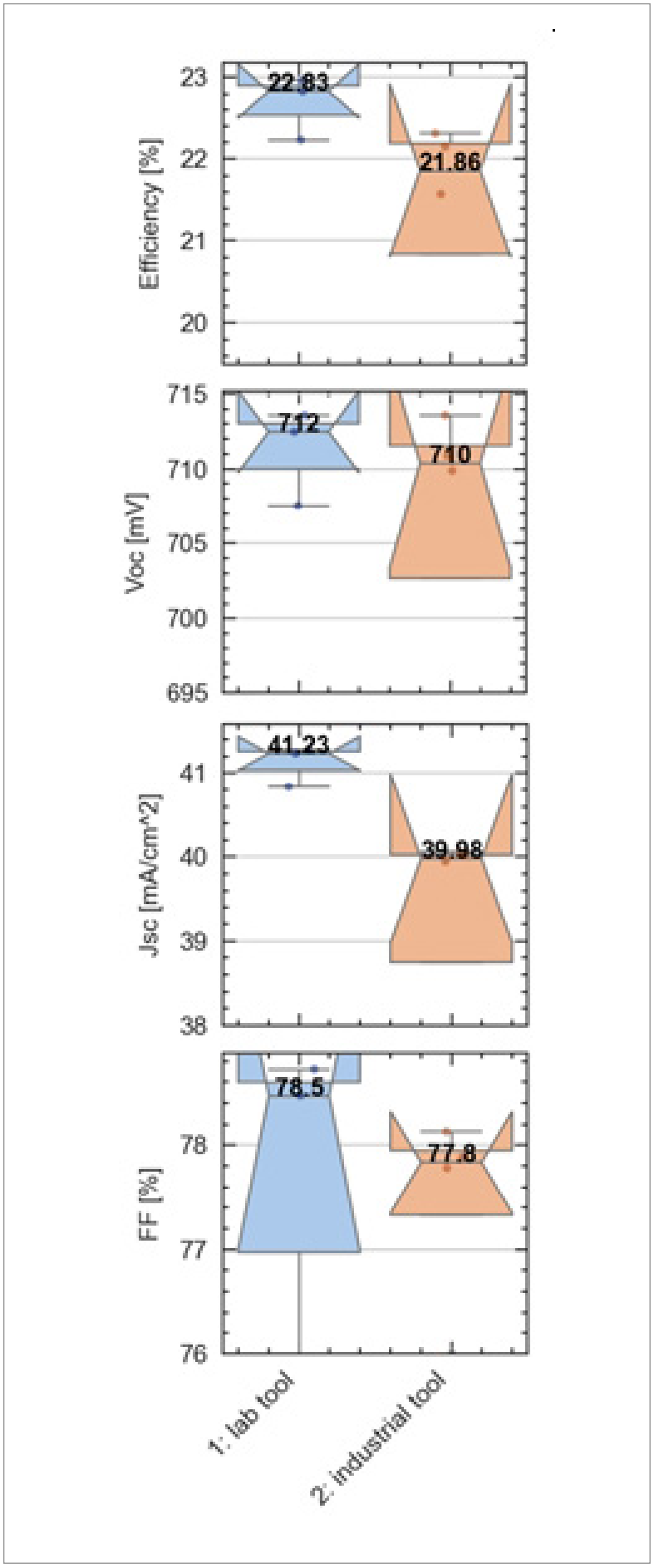

IV parameters of POLO IBC cells with local PECVD deposition through a shadow mask using either the lab-type or industrial tool.

"…. we expect that the conversion efficiencies obtained with the industrial tool will approach the values obtained with the lab tool"

Using the ISC Konstanz cost model, we calculate that POLO IBC modules will produce electricity in utility-scale (and residential) applications ca. 4% (and ca. 7%) cheaper compared to PERC+ modules, since the 9%rel higher cell efficiency will substantially reduce the area-related balance of system costs per kWp. Hence, this POLO IBC technology is attractive for new cell production lines as well as for upgrading PERC+ fabs to POLO IBC with minimal conversion investment.

Conclusion

In this paper, we demonstrated a novel manufacturing process sequence for POLO IBC solar cells by applying a local PECVD SiO_xN_y/n-a-Si deposition through a glass shadow mask to form the structured carrier-selective n-poly-Si layer in a single process step. After developing the process using a lab-type tool, we transferred the PECVD SiO_xN_y/n-a-Si to an industrial c.plasma tool and obtained an excellent J_o of 3 fA/cm² after firing. Fully processed POLO IBC solar cells on M2-sized Ga-doped Cz wafers exhibited conversion efficiencies of up to 23.0% with Voc = 708 mV, J_{sc} = 41.2 mA/cm² and *FF* = 78.7% when processed with the lab PECVD tool, alongside an excellent iVoc of 741 mV. We attribute the 33 mV difference between iVoc and Voc to additional J_o contributions of the Ag and Al metal contacts, which is subject to future improvements. The first POLO IBC solar cells processed with the c.plasma tool with shadow masks achieved conversion efficiencies of up to 22.3% and average Voc values of 710 mV. As next steps towards production readiness, we aim at further increasing the conversion efficiency towards 25% and implementing an automated shadow mask loading into the industrial c.plasma tool.

Acknowledgements

We gratefully acknowledge the support of the German Federal Ministry for Economic Affairs and Climate Action under the contracts 03EE1098 and 03EE1102E.

References

[1] International Technology Roadmap for Photovoltaic (ITRPV), 13th Edition, 2022.
[2] T. Dullweber et al., Evolutionary PERC+ solar cell efficiency projection towards 24% evaluating shadow-mask-deposited poly-Si fingers below the

	PERC+	POLO-IBC
Cell Efficiency	**23.00%**	**25.00%**
	USDct/Wp	USDct/Wp
KOH batch texture	0.52	0.48
P-Diffusion	0.27	
Edge isolation and PSG removal SSE	0.56	0.52
PECVD SiON/na-Si with shadow mask		0.40
Anneal /SiO2 or Anneal N2	0.15	0.20
PECVD SiNx/AIOx	0.49	0.45
PECVD SiNx/AIOx/SiNx	0.43	0.45
Laser SiNx ablation	0.09	0.09
Printing 4 Stage (w/o paste cost)	1.12	1.03
pure Ag cost USD/cell	0.88	1.01
Total cell processing cost (w/o wafer)	**4.51**	**4.62**

Figure 7: Cost-of-ownership calculations of POLO IBC versus PERC+ cell process costs, applying a cost model from ISC Konstanz. Whereas the cell processing costs are comparable, we expect that the levelized cost of electricity (LCOE) of POLO IBC modules in utility-scale (residential) applications will be up to 4% (7%) cheaper due to the higher conversion efficiency potential.

Ag front contact as next improvement step. Sol. Energy Mater. Sol. Cells (2020), vol. 212, No. 110586.
[3] R. Brendel et al., Recent Progress and Options for Future Crystalline Silicon Solar Cells, Proceedings 28th European Photovoltaic Solar Energy Conference (2013), pp. 676–690.
[4] F. Haase et al., Transferring the record p-type Si POLO-IBC cell technology towards an industrial level, Proceedings 46th IEEE PVSC, Chicago, IL, USA (2019). pp. 2200–2206.
[5] F. Feldmann et al., A passivated rear contact for high-efficiency n-type Si solar cells enabling high Voc's and *FF* > 82%, Proceedings 28th European Photovoltaic Solar Energy Conference (2013), pp. 988–992.
[6] C.N. Kruse et al., Simulation-based roadmap for the integration of poly-silicon on oxide contacts into screen-printed crystalline silicon solar cells. Sci. Rep. (2021), vol. 11, No. 996.
[7] M. Stöhr et al., Firing-Stable PECVD SiO_xN_y/n-Poly-Si Surface Passivation for Silicon Solar Cells, ACS Appl. Energy Mater. (2021), 4 (5), 4646–4653.
[8] M. Stoehr et al., PECVD shadow mask deposition of amorphous silicon – a short cut to local passivating contacts, 37th European Photovoltaic Solar Energy Conference (2020), pp. 521–524.
[9] T. Dullweber et al., presented at SNEC (2021).
[10] V. Mertens et al., Local PECVD SION/n-poly-Si deposition through a shadow mask for POLO IBC solar cells, Proceedings 38th European Photovoltaic Solar Energy Conference (2021), pp. 135–139.
[11] T. Dullweber et al., Towards cost-effective high-efficiency POLO IBC solar cells with minimal conversion invest for existing PERC+ production lines, Proceedings 8th World Conf. Photovolt. Energy Conversion (2022), in press.
[12] S. Gatz et al., Firing stability of SiN_y/SiN_x stacks for the surface passivation of crystalline silicon solar cells, Sol. Energy Mater. Sol. Cells (2012), vol. 96, pp. 180–185.

Enquiries

Thorsten Dullweber
Institute for Solar Energy Research Hamelin (ISFH),
Am Ohrberg 1,
31860 Emmerthal, Germany

Email: dullweber@isfh.de
Tel: +49 (0)5151-642